

Invited Lecture at ISROMAC 12,
Twelfth International Symposium on Transport Phenomena and Dynamics of Rotating Machinery,
Honolulu, Hawaii, Feb.17-22, 2008

CLOUD CAVITATION WITH PARTICULAR ATTENTION TO PUMPS

Christopher E. Brennen
California Institute of Technology,
Pasadena, California 91125

ABSTRACT

In many cavitating liquid flows, when the number and concentration of the bubbles exceeds some critical level, the flow becomes unsteady and large clouds of cavitating bubbles are periodically formed and then collapse when convected into regions of higher pressure. This phenomenon is known as cloud cavitation and when it occurs it is almost always associated with a substantial increase in the cavitation noise and damage. These increases represent serious problems in devices as disparate as marine propellers, cavitating pumps and artificial heart valves. This lecture will present a brief review of the analyses of cloud cavitation in simplified geometries that allow us to anticipate the behavior of clouds of cavitation bubbles and the parameters that influence that behaviour. These simpler geometries allow some anticipation of the role of cloud cavitation in more complicated flows such as those in cavitating pumps.

1 Introduction

It has become abundantly clear in recent years that knowledge of the dynamics and acoustics of bubble clouds (as opposed to single bubbles) is essential to our understanding of a very broad range of physical effects involving bubbles. For example, the collapse of clouds of cavitation bubbles often results in much greater noise and damage than would result from the sum of the effects of individual bubbles. In the context of cavitating propellers or turbomachines this is a cause for grave concern and the lack of understanding of the processes of periodic formation and collapse of cavitation clouds remains a key issue. Similar concerns surround the formation of clouds of cavitation bubbles in contexts as diverse as artificial heart valves or the earthquake-induced cavitation effects on dams. But there are also contexts in which these cloud effects can be an advantage such as in the destruction of kidney stones by lithotripsy.

In this paper we give a very brief account of analyses that provide our current understanding of the dynamics of cavitation clouds. This will be followed by several examples of experimental observations of cloud cavitation in water tunnel experiments and in pump tests.

2 Review of bubble cloud effects

2.1 Natural frequencies

Though the first analysis that indicated how bubbles might behave collectively was conducted by van Wijngaarden (1964) on a plane layer of bubbles next to a wall, it is more convenient to focus attention on a finite spherical cloud surrounded by pure liquid and to briefly review the dynamics and acoustics of such a cloud. We begin with the simplified case shown in figure 1 in which all the bubbles in the cloud have the same equilibrium size, R_0 , and are uniformly distributed within the cloud. Thus the population as represented by the initial equilibrium void fraction, α_0 , is uniform within the cloud. Radial position within the cloud is denoted by r and the initial radius of the cloud by A_0 .

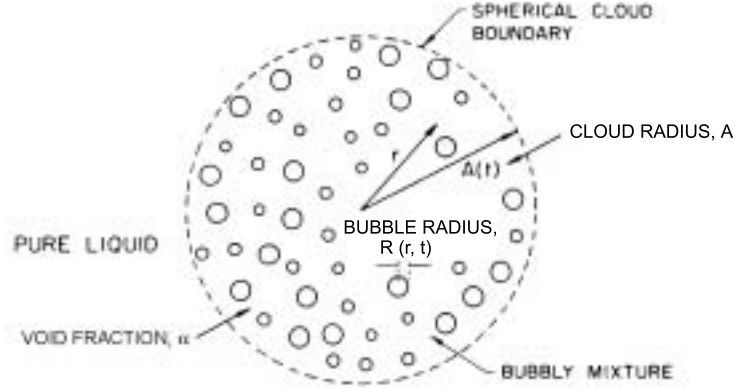


Figure 1: Spherical cloud of bubbles: notation.

d’Agostino and Brennen (1983, 1989) showed that a linearized dynamics analysis of such a cloud reveals that it has its own, infinite set of natural frequencies denoted by ω_n and given by

$$\omega_n = \omega_N \left[1 + \frac{4}{3\pi^2(2n-1)^2} \frac{A_0^2}{R_0^2} \frac{\alpha_0}{1-\alpha_0} \right]^{-\frac{1}{2}} ; n = 1, 2, \dots \quad \text{and} \quad \omega_\infty = \omega_N \quad (1)$$

where ω_N is the natural frequency of an individual bubble oscillating alone in an infinite liquid. The above is an infinite series of frequencies of which ω_1 is the lowest. The higher frequencies approach ω_N as n tends to infinity. As expected these natural frequencies correspond to modes with more and more nodes as n increases (see Brennen 1995). Note in particular that the lowest natural frequency, ω_1 , is given by

$$\omega_1 = \omega_N \left[1 + \frac{4}{3\pi^2} \frac{A_0^2}{R_0^2} \frac{\alpha_0}{1-\alpha_0} \right]^{-\frac{1}{2}} \quad (2)$$

Note also that this can be much smaller than ω_N if the initial void fraction, α_0 , is much larger than the square of the ratio of bubble size to cloud size ($\alpha_0 \gg R_0^2/A_0^2$). If the reverse is the case ($\alpha_0 \ll R_0^2/A_0^2$), all the natural frequencies of the cloud are contained in a small range just below ω_N . This defines a special parameter, $\beta = \alpha_0 A_0^2/R_0^2$, that governs the cloud interaction effects and that is termed the “Cloud Interaction Parameter”. If $\beta \ll 1$ there is relatively little bubble interaction effect and all the bubbles oscillate at close to the frequency, ω_N , as if each were surrounded by nothing but liquid. On the other hand when $\beta > 1$ the cloud has natural frequencies much less than ω_N and there are strong interaction effects between the bubbles in the cloud. Note that in various applications the magnitude of β could take a wide range of values from much less than unity to much greater than unity. It will be small in small clouds with a few large bubbles and a low void fraction but could be large in large clouds of small bubbles with higher void fraction.

2.2 Linear dynamics of a simple cloud

Further exploration of the forced linearized response of a cloud to oscillations in the pressure in the liquid far from the bubble (d’Agostino and Brennen 1983, 1989) reveals the following characteristics. In the absence of damping in the Rayleigh-Plesset equation for the bubble dynamics, infinite peaks in the response occur at all the natural frequencies as shown in figure 2. However, when a reasonable estimate of the damping is included (d’Agostino and Brennen 1989), the attenuation of the higher frequencies is much greater so the dominant peak in the response occurs at the lowest natural frequency of the cloud, ω_1 . The response at

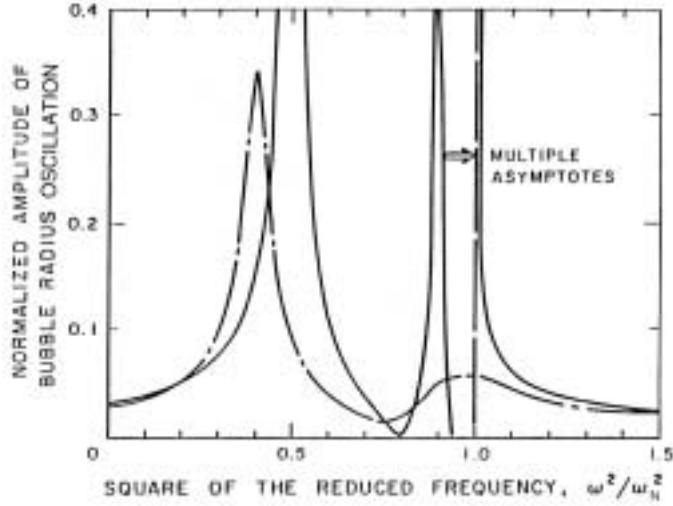


Figure 2: The amplitude of the bubble radius oscillation at the cloud surface as a function of frequency (for the case of $\beta \approx 0.8$). Solid line is without damping; broken line includes damping. From d’Agostino and Brennen (1989).

Figure 3: The amplitude of the bubble radius oscillation at the cloud surface as a function of frequency for damped oscillations at three values of $\beta \approx 0.8$ (solid line), $\beta \approx 0.4$ (dot-dash line), and $\beta \approx 1.65$ (dashed line). From d’Agostino and Brennen (1989).

the bubble natural frequency, ω_N , becomes much less significant. The effect of varying the cloud interaction parameter, β , is shown in figure 3, where the amplitude of bubble radius oscillation at the cloud surface is presented as a function of ω . Note that increasing β causes a reduction in both the amplitude and frequency of the dominant response at the lowest natural frequency of the cloud. It is important to emphasize that the results presented above are linear and that there are very significant nonlinear effects that we now proceed to describe. In addition we have focused exclusively on spherical bubble clouds since solutions of the basic equations for other, more complex geometries are not readily obtained. However, d’Agostino et al. (1988) have examined some of the characteristics of this class of bubbly flows past slender bodies (for example, the flow over a wavy surface).

2.3 Cavitation of a spherical cloud

If a spherical cloud is subjected to an episode of sufficiently low pressure it will cavitate, in other words the bubbles will grow explosively to many times their original size. Subsequently, if the pressure far from the cloud increases again (as, for example, when the cloud is convected out of the region of low pressure) the bubbles will collapse violently. The reaction of a single bubble to such a low pressure episode has, of course, been studied extensively; typically the Rayleigh-Plesset equation is used to model the highly non-linear reaction of the single bubble. However, the response of a cloud of bubbles is more complex. A valuable perspective on the subject was that introduced by Mørch (1980, 1981, 1982) and Hanson, Kedrinskii and Mørch (1981). They suggested that the collapse of a cloud of bubbles involves the formation and inward propagation of a shock wave and that the geometric focusing of this shock at the center of cloud creates the enhancement of the noise and damage potential associated with cloud collapse. Wang and Brennen (1995a, b) and Reisman *et al* (1998) employed the use of continuity and momentum equations coupled to the Rayleigh-Plesset equation in order to model the two-phase flow within the cloud. Here we briefly review their numerical calculations that detailed the dynamics of a spherical cloud of cavitating bubbles. (Previous

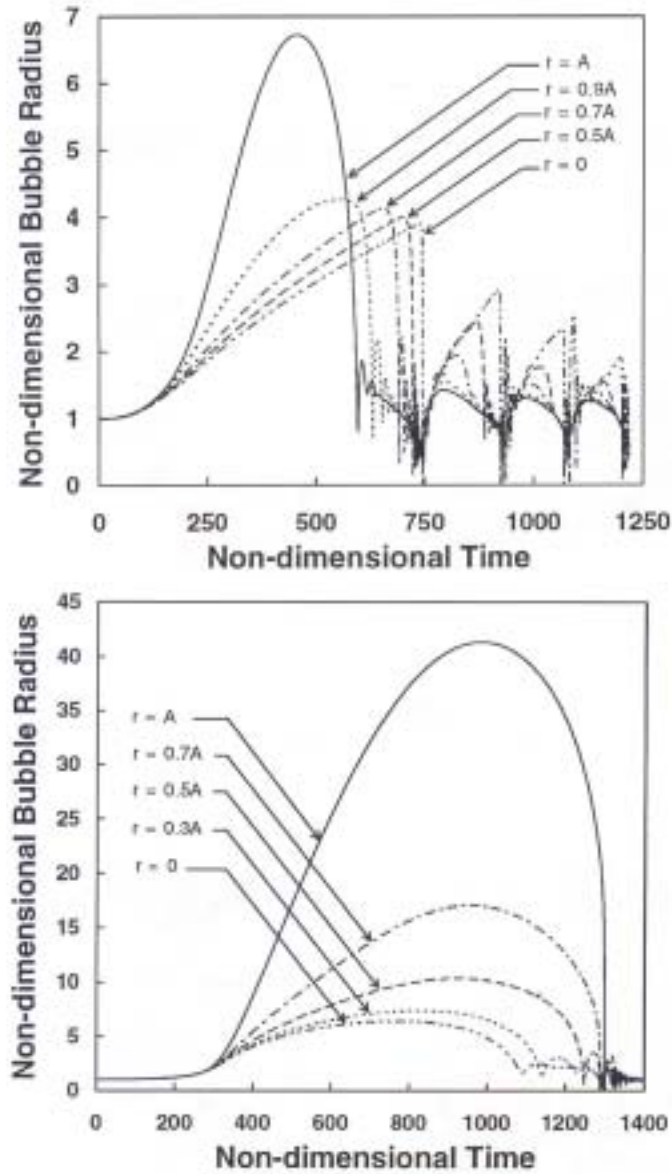


Figure 4: Typical time histories of the bubble size at six different Lagrangian positions in a spherical cloud in response to an episode of reduced pressure in the surrounding liquid (between $t=0$ and $t=250$). The upper figure is for $\beta \gg 1$ while the lower graph is for β of order unity. From Wang and Brennen (1995).

numerical investigations of the nonlinear dynamics of cavity clouds were carried out by Chahine (1982), Omta (1987), and Kumar and Brennen (1991, 1992, 1993)).

It transpires that the response of a cloud to an episode of reduced pressure in the surrounding liquid is quite different depending on the magnitude of β . When β is much greater than unity the typical cloud response to an episode of reduced pressure is shown in figure 4(upper). Note that the bubbles on the surface of the cloud grow more rapidly than those in the interior which are effectively shielded from the reduced pressure in the surrounding liquid. More importantly the bubbles on the surface collapse first and a collapse front propagates inward from the cloud surface developing into a substantial shock wave. Due to geometric

focusing this shock wave strengthens as the shock proceeds inwards and creates a very large pressure pulse when it reached the center of the cloud. On the other hand when β is small, the response of the cloud is quite different as shown in figure 4(lower). Then the bubbles at the center of the cloud to collapse first, resulting in an outgoing collapse front that weakens geometrically resulting in a quite different and much more benign dynamic.

While real bubble clouds are often far from spherical the potential for similar shielding effects still clearly exist and below we will describe some experimental observations of shocks in collapsing bubble clouds.

3 Experimental Observations

3.1 Past Observations

The highly destructive consequences of cloud cavitation have been known for a long time and have been documented, for example, by Knapp (1955), Bark and van Berlekom (1978) and Soyama *et al.* (1992). The generation of these cavitation clouds may occur naturally as a result of the shedding of bubble-filled vortices, or it may be the response to a periodic disturbance imposed on the flow. Common examples of imposed fluctuations are the interaction between rotor and stator blades in a pump or turbine and the interaction between a ship's propeller and the non-uniform wake created by the hull. As a result numerous investigators (for example, Wade and Acosta 1966, Bark and van Berlekom 1978, Shen and Peterson 1978, 1980, Bark 1985, Franc and Michel 1988, Hart *et al.* 1990, Kubota *et al.* 1989, 1992, Le *et al.* 1993, de Lange *et al.* 1994) have studied the complicated flow patterns involved in the production and collapse of cloud cavitation on a hydrofoil. The radiated noise produced is characterized by pressure pulses of very short duration and large magnitude. These pressure pulses have been measured by Bark (1985), Bark and van Berlekom (1978), Le *et al.* (1993), Shen and Peterson (1978, 1980) and McKenney and Brennen (1994).

3.2 Some experimental observations using an oscillating hydrofoil

We describe here some experimental observations of Reisman *et al.* (1998) who deployed an oscillating hydrofoil in a water tunnel to produce regular clouds of cavitation whose behavior could then be observed and measured. Several finite span hydrofoils with a rectangular planform were reflection-plane mounted in the floor of a water tunnel test section and, as described in Reisman *et al.* (1998), were driven in an oscillatory pitching motion with frequencies up to $50Hz$ and incidence angle amplitudes of the order of $5 - 10^\circ$. One of the hydrofoils was equipped with flush-mounted surface pressure transducers located at 26% span from the foil base and 30%, 50%, 70% and 90% chord from the leading edge (denoted respectively by #1 through #4). Additional dynamic transducers were located on the nearby tunnel walls. High speed motion pictures (taken at $500fps$) allowed examination of the processes of formation, growth and collapse of a cloud of cavitation bubble during each cycle of the hydrofoil oscillation. During the part of the oscillation cycle when the incidence angle is increasing, cavitation inception occurs in the tip vortex and is soon followed by traveling bubble cavitation on the suction surface. As the angle of attack increases further, the bubbles coalesce into a single attached cavitation sheet; near the end of this process, a re-entrant liquid jet penetrates the attached cavity from downstream and causes the break-up into a cloud of bubbles. This cloud then detaches from the hydrofoil and collapses catastrophically as it is being convected downstream. All of the substantial radiated noise occurred during this bubbly collapse part of the cycle. It consisted of pressure pulses of very short duration and large magnitude that were qualitatively similar to those measured by Bark (1985), Bark and van Berlekom (1978), Le *et al.* (1993) and Shen and Peterson (1978, 1980).

This so-called "global" collapse is illustrated by the four successive movie frames included in figure 5. The global cloud collapse occurs between frames (b) and (c). Note that this collapse results in only a slight change in the cloud radius but a large change in the void fraction magnitude and distribution inside the cloud, an observation that is consistent with the previously described calculations of Wang and Brennen.

Reisman *et al.* (1998) correlated the movies with the transducer pressure measurements and found that the pressure pulses recorded (both on the foil surface and in the far field) were clearly associated with specific

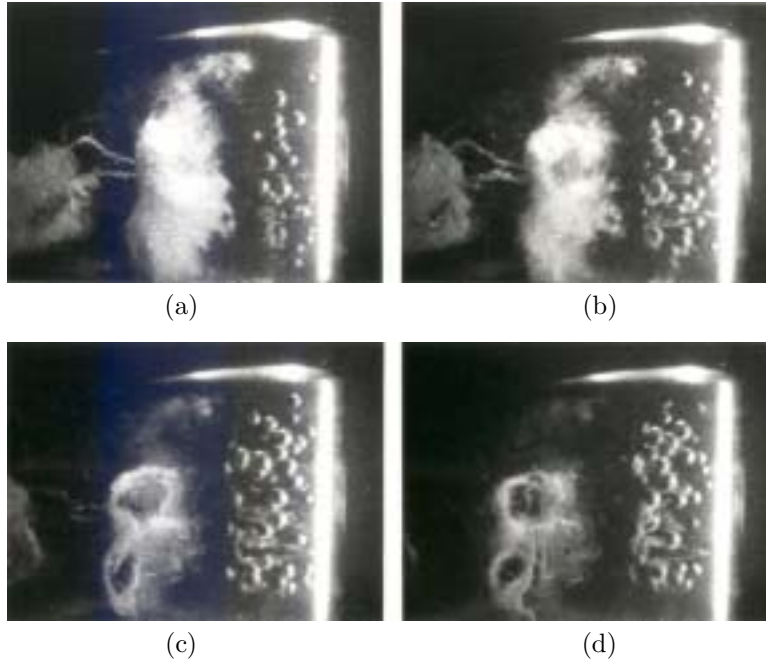


Figure 5: Example of consecutive high speed movie frames ($2ms$ apart) of the collapse of a cloud of cavitation bubbles on the suction surface of a hydrofoil. The flow is from right to left. A global cloud collapse occurs between frames (b) and (c). From Reisman *et al.* (1998).

structures (more precisely, the dynamics of specific structures) which are visible in the movies. Indeed, it appears that several types of propagating structures (shock waves) are formed in the collapsing cloud and dictate the dynamics and acoustics of collapse.

A typical set of transducer recordings is shown in figure 6 which represents a single foil oscillation cycle with the origin corresponding to the maximum angle of attack. The signals are characterized by very large amplitude pressure pulses with magnitudes of the order of tens of atmospheres and typical durations of the order of tenths of milliseconds. Note that the radiated, far-field acoustic pressure recorded by the floor and ceiling transducers also contains pulses and these are exemplified by the bottom trace in figure 6. The magnitude of the pulses measured by the transducer in the tunnel floor is on the order of one atmosphere. [The low frequency variation present in the signal prior is the result of stresses and accelerations of the hydrofoil rather than pressure variations.]

In the experiments, two different types of pressure pulses were identified and can be illustrated by figure 6. The pulses occurring before the $0.04s$ mark are randomly distributed in time and space and are not repeated from cycle to cycle. These will be referred to as *local* pulses. On the other hand, the pulses located between $0.04s$ and $0.05s$ occur virtually simultaneously, are of higher amplitude and are repeated each cycle. These *global* pulses were readily correlated with the visual observations of the coherent global collapse of the well-defined bubble clouds described above. They produced substantial far-field noise.

But, unexpectedly, two other types of structures were observed. Typically, their pulses are recorded by only one transducer as exemplified by the individual pulses in figure 6 occurring before the $0.04s$ mark. These are randomly distributed in time and space and are not repeated from cycle to cycle. They are referred to as *local* pulses. (In contrast the global pulses located between $0.04s$ and $0.05s$ occur virtually simultaneously, are of higher amplitude and are repeated each cycle.) While these *local* events are smaller and therefore produce less radiated noise, the pressure pulse magnitudes are almost as large as those produced by *global* events.

Correlation of the high-speed movies with the transducer output revealed that local pulses occurred

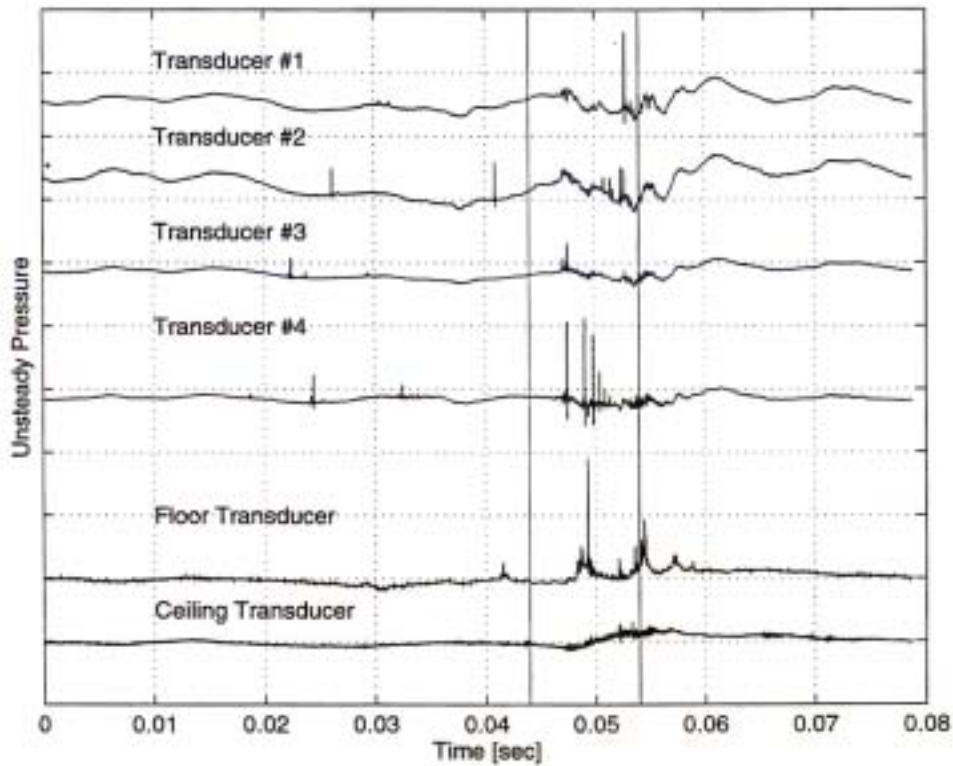


Figure 6: Typical signals from the transducers during a single cycle of foil oscillation. The vertical scale is 1 MPa/div. for the hydrofoil surface transducers, #1-#4, and 100 kPa/div. for the floor and ceiling transducers. From Reisman *et al.* (1998).

when one of two particular types of flow structures passed over the face of a transducer. The two types of structures will be referred to as “crescent-shaped regions” and “leading edge structures”; both occur during the less coherent collapse of clouds. Crescent-shaped regions are illustrated in photographs (a) through (c) of figure 7) and careful correlation revealed that the passage of one of these over an individual transducer produced a large local pulse in the output of that transducer. A crescent-shaped region has a low void fraction and, consequently, must involve a substantial compression pulse at its leading edge. These crescent-shaped regions appear randomly and ephemerally in the bubbly mixture. A close look at photograph (c) shows how complicated these flow structures can be since this crescent-shaped region appears to have some internal structure. Photographs (b) and (c) show that more than one crescent-shaped structure can be present at any moment in time.

In addition, the movie and pressure data consistently displayed a local pulse when the upstream boundary, or leading edge, of the detached bubbly mixture passed over a transducer. This second type of local flow structure is illustrated in photograph (d) of figure 7 and also produces a local pulse. These “leading edge structures” are created when the mixture detaches from the foil; they propagate downstream faster than the mixture velocity.

Parenthetically, we note that injection of air into the cavitation on the suction surface can substantially reduce the magnitude of the pressure pulses produced (Ukon 1986, Arndt *et al.* 1993, Reisman *et al.* 1997). However Reisman *et al.* (1997) have shown that the bubbly shock wave structures still occur; but with the additional air content in the bubbles, the pressure pulses are substantially reduced.

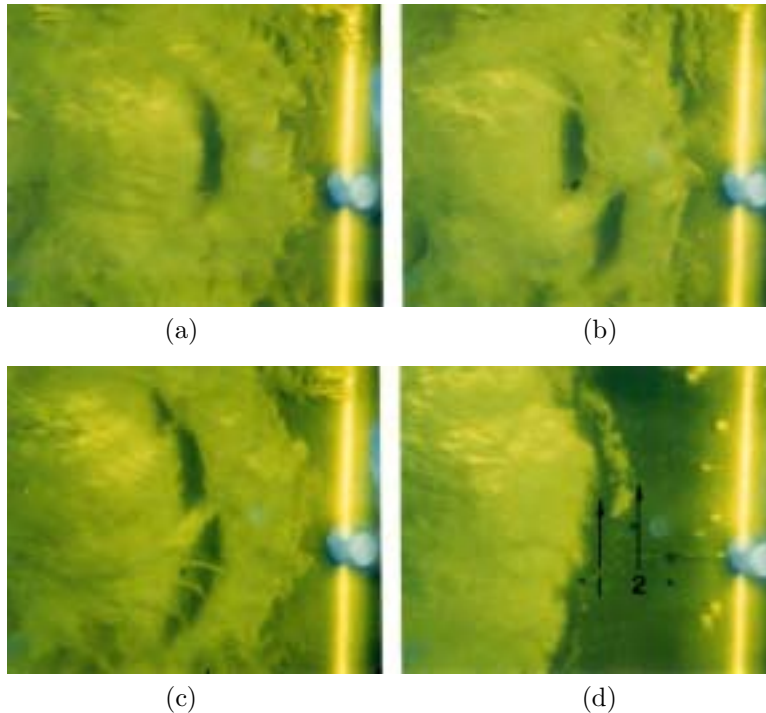


Figure 7: Local pulse structures in the cavitation on the suction surface of a cavitating foil. The flow is from right to left. Crescent-shaped structures are seen in (a), (b), and (c) and a leading edge event with two collapses is shown in photograph (d). From Reisman *et al.* (1998).

Finally we note that pulses like those measured on the surface of the hydrofoil with typical magnitudes as large as 10bar and durations of the order of 10^{-4}s are certainly sufficient to explain the enhanced noise and cavitation damage associated with cloud cavitation.

3.3 Some observations in a centrifugal pump

The author was asked to investigate a particular case of a centrifugal wastewater pump that was exhibiting substantial vibration levels at higher run speeds and, in the course of this investigation, gathered significant vibration data that suggests substantial cloud cavitation involvement at higher speeds due to interaction between the impeller vanes and the volute cutwater. The pump was a vertical-axis, variable-speed, single volute pump with a 13.81in diameter, three-vaned impeller designed to run at speeds up to about 700rpm . The design included a suction line with a 90° elbow immediately upstream of the pump suction. The pump was intended for operation at a flow coefficient (based on impeller discharge flow area and tip speed) of 0.079 and a head coefficient of 0.425 . Under these maximum speed conditions the available NPSH meant a suction specific speed, S , of about 5860 . As could have been anticipated, this S meant that the pump cavitated but that the limited cavitation did not produce significant cavitation head loss. Measurements confirmed this lack of significant cavitation head loss. However, the vibration levels were much greater than expected and exhibited the following characteristics.

The pump(s) were instrumented with high fidelity accelerometers on the bearing housing just above the pump and both static and dynamic pressure transducers on the pump suction and discharge. Data was obtained for a range of speeds from 420rpm to about 680rpm , all at roughly the same NPSH. (Data was also taken with an without the injection of air at the suction flange, in one (vain) effort to reduce the vibration level substantially.) Though no cavitation head loss occurred, the vibration changed substantially

in amplitude and character as the speed was increased so that the overall vibration level exceeded the *ISO10816* satisfactory vibration limit of $0.177ips - rms$ for all speeds above $550rpm$. We focus here on those vibration characteristics and the associated pressure oscillations. It should also be noted that the noise level varied somewhat over time since cavitation is dependent on the debris in the wastewater and this drifted up and down with time during the tests.

During all tests the author monitored the pump noise at various points on the pump volute, suction and discharge lines using a mechanics stethoscope. The following observations were made:

1. At low speeds (below $540rpm$) the cavitation noise was minor and relatively constant and continuous, a high frequency hissing sound superimposed on the mechanical noise. Its magnitude, both in absolute terms and relative to the mechanical noise, increased significantly with speed within this low speed range. This noise was always substantially attenuated with just the smallest air injection rate of $0.1scfm$ and some further reduction occurred at higher air flow rates.
2. At higher speeds (greater than $540rpm$), a different and much more violent noise begins to dominate. This begins as a crackling and transitions into a severe banging as the speed is increased. This noise has a dominant blade passage frequency component at three times the rotational frequency. Low levels of air injection (0.1 to $0.5scfm$) caused some minor muting of this low frequency banging. Further reduction occurs with increasing air injection (up to the maximum tested namely $10scfm$) but the benefits become less and less and the level of the banging noise seems to asymptote to a level independent of the air injection rate.
3. Two different (but single) injection locations were tested but the differences were minor.

It should be noted that there is documentation in the literature which indicates that cavitation noise level (usually defined at the high frequency hissing noise) can be utilized as an approximate, qualitative measure of the rate of cavitation damage within a particular pump. As far as the author is aware these studies pertain to well designed pumps that do not manifest the extreme banging noise generated in these tests.

In the higher speed range typical vibration spectra from the accelerometers (for each of the three directions) is shown in figure 8. The dominant contribution to the vibration is at the fundamental vane passing frequency (or three times the rotational frequency or $3/rev$ for short) with an additional notable peak at twice the vane passing frequency ($6/rev$ for short). The magnitude of the $3/rev$ peak increased fairly monotonically with speed as shown in figure 9.

The spectra from the pressure transducers contained similar components though the peaks at $6/rev$ were often larger than those at the fundamental $3/rev$ frequency as exemplified by the discharge pressure spectra shown in figure 10. This strongly suggests a highly non-linear vane/cutwater interaction consisting of a short pulse with each interaction that yields stronger higher harmonics in the pressure pulsations and thus a larger $6/rev$ peak. However, higher frequencies will be more highly attenuated as the oscillations are transmitted through the structure to the accelerometers and consequently the $6/rev$ frequency is not so dominant in the accelerometer spectra. This is consistent with the rapid collapse of a cavitation cloud following each vane/cutwater interaction.

Finally we summarize the effects of injecting air into the flow at one point around the suction flange. In the lower speed range (less than $550rpm$) a small amount of air injection (less than $1scfm$) produced a modest decrease of roughly 15% decrease in the overall vibration level mostly by decreasing the high frequency "hissing" noise. Larger air injection rates generated little additional benefit. In the higher speed range, above $600rpm$, the effect of air injection is still measurable but the effect on the banging is very modest. An average 14% decrease in the overall vibration is produced by air injection rates up to $10scfm$. However, the resulting vibration with any amount of air injection was still greater than the *ISO 10816* vibration limits.

The main effect of air injection was to change the spectra of the oscillations rather than the magnitude. Figure 10 illustrates the dramatic change in the discharge pressure spectra that occurs between air injection rates of zero and $10scfm$. When the air injection rate is increased beyond about $1scfm$, for example to

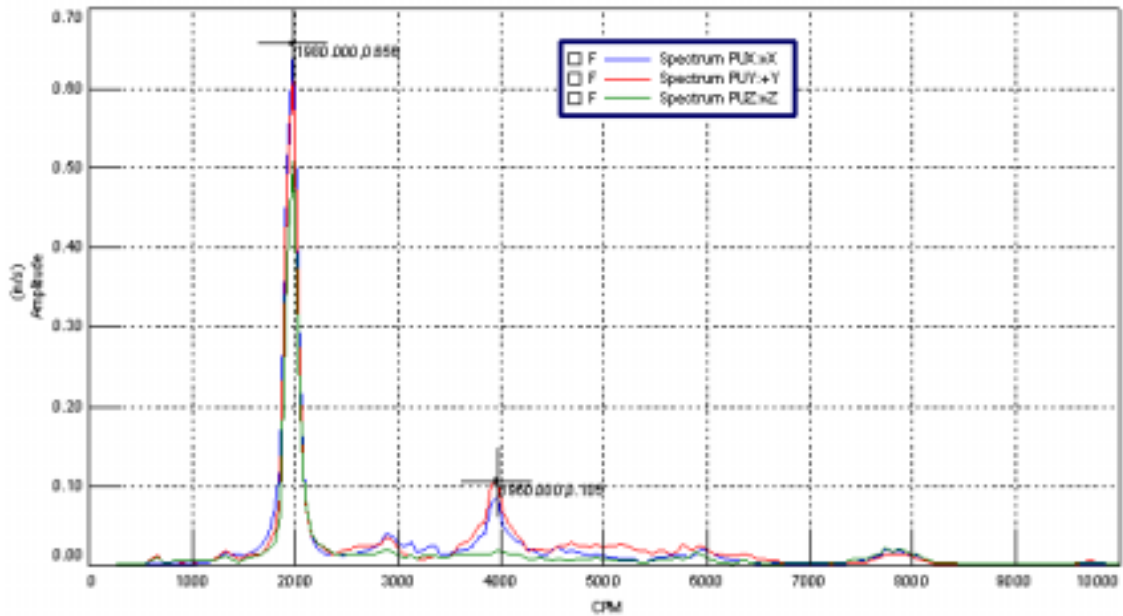


Figure 8: Accelerometer spectra for three different directions at 655rpm. The blue and red lines are the horizontal components, green is the vertical component.

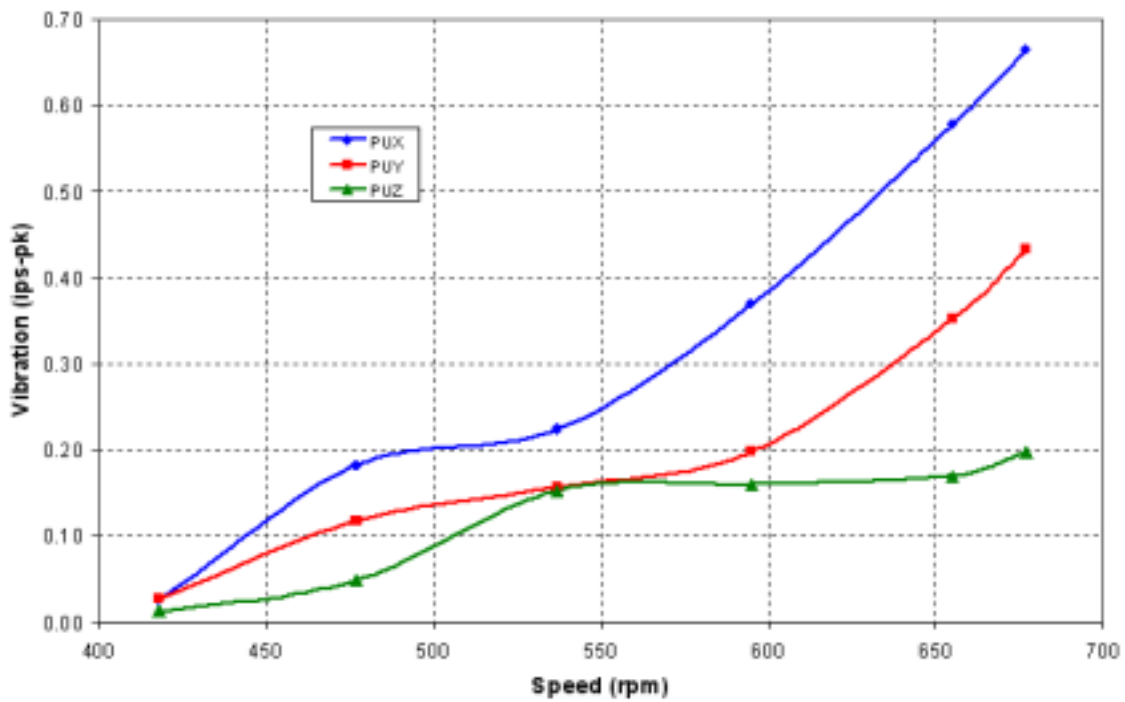


Figure 9: The magnitude of the accelerometer signal component vane passing frequency peak as a function of speed. The blue and red lines are the horizontal components, green is the vertical component.

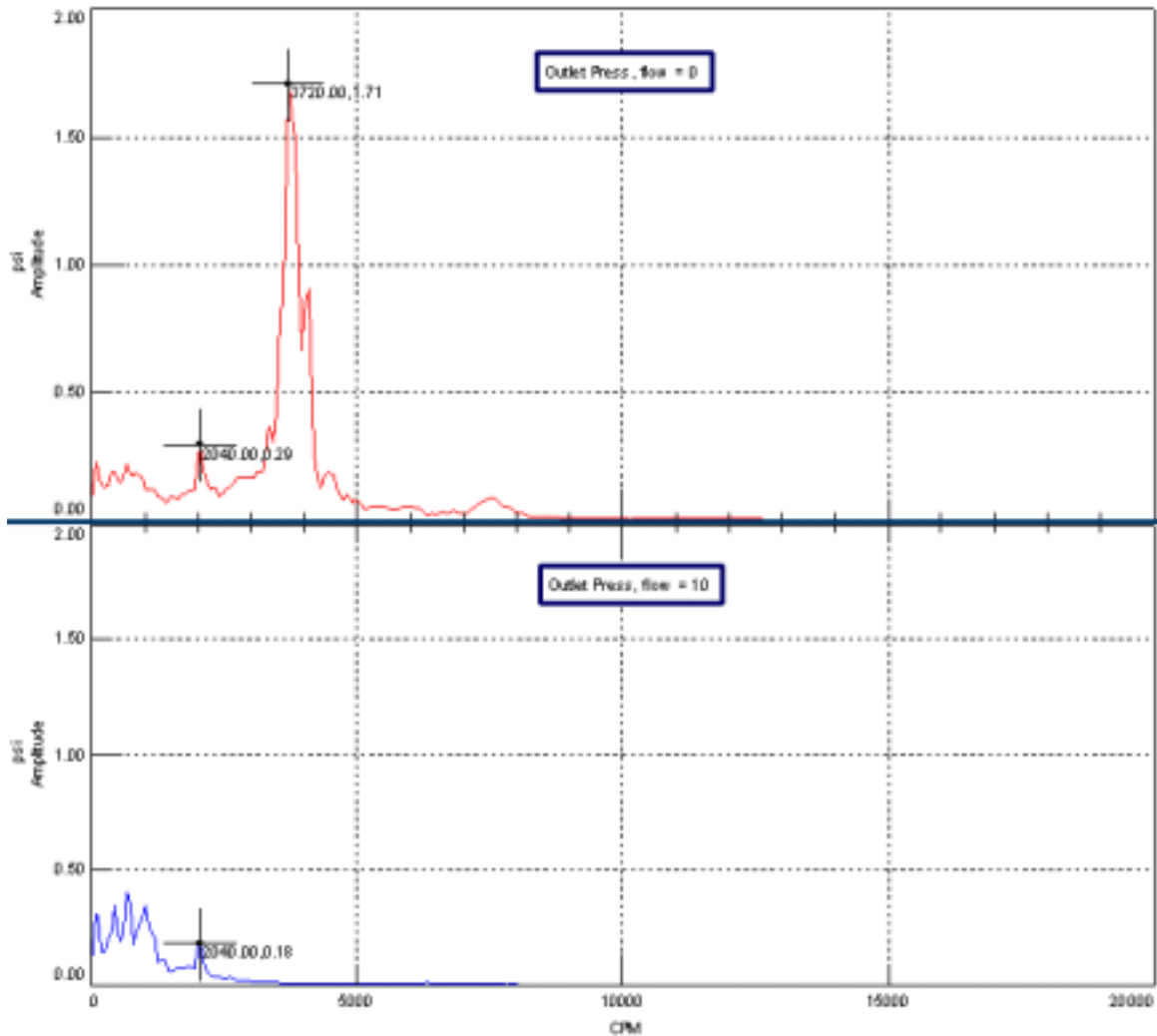


Figure 10: Typical discharge pressure spectra at $677rpm$ and at two air injection flows, zero (upper graph) and $10scfm$ (lower graph).

the $10scfm$ level of lower plot in figure 10, the 6/rev pressure oscillation is essentially eliminated and even the 3/rev component is reduced. Further illustration of these effects is provided in figure 11 which plots the change in the magnitudes of the 3/rev and 6/rev peaks as the air injection rate is increased. Note that at air injection rates less than $1scfm$, there is essentially no change in the amplitudes. Between $1scfm$ and $3scfm$, there is a substantial decrease in both components.

As illustrated in figure 10, the 3/rev and 6/rev peaks are largely replaced by a group of lower frequencies clustered around the rotation frequency and with amplitudes higher than in the absence of air injection. These correspond to the low-frequency “banging” described earlier. This is consistent with bubble clouds that have a higher bubble density, a higher void fraction and/or lower frequency bubbles containing more air. arewould base correspond

While the evidence is not completely conclusive, all of the above features of the excessive vibration in this pump are consistent with the periodic formation and collapse of a cavitation cloud at each impeller vane/cutwater encounter. It seems likely that this interaction is amplified by the small number of vanes and

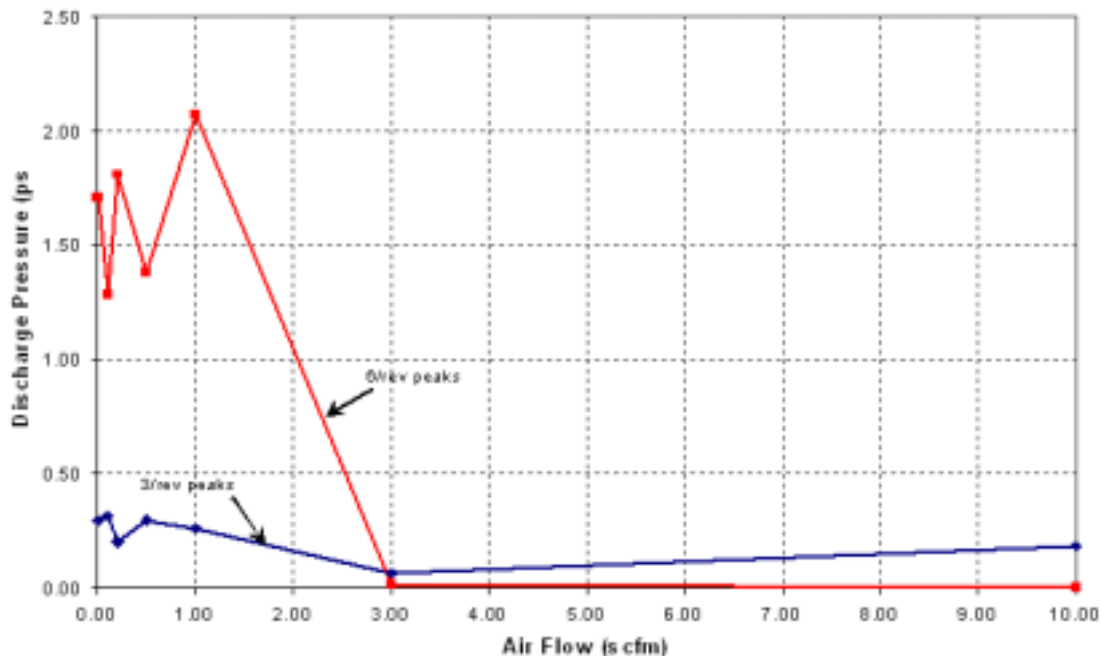


Figure 11: Discharge pressure components on Pump #2 as a function of air injection at 677rpm.

a flow incidence mismatch at the volute cutwater. An attempt to ameliorate the vibration by injection of air was largely unsuccessful but produced a significant downshift in the dominant frequencies that would be consistent with clouds with a larger void fraction and bubbles and clouds with lower resonant frequencies.

4 Concluding Comments

In this paper we have summarized some of the recent advances in our understanding of bubbly cloud cavitation. It has become clear that effects due to the interaction between bubbles may be crucially important especially when they give rise to the phenomenon called cloud cavitation. Calculations of the growth and collapse of a spherical cloud of cavitating bubbles show that when the cloud interaction parameter (β) is large enough, collapse occurs first on the surface of the cloud. As was anticipated by the work of Mørch, Kedrinskii and Hanson (Mørch 1980, 1981, 1982 and Hanson *et al.* 1981), the inward propagating collapse front becomes a bubbly shock wave which grows in magnitude due to geometric focussing. Very large pressures and radiated impulses occur when this shock wave reaches the center of the cloud.

Of course, actual clouds are far from spherical. And, even in a homogeneous medium, gasdynamic shock focussing can be quite complex and involve significant non-linear effects (see, for example, Sturtevant and Kulkarny 1976). Nevertheless, it seems evident that once collapse is initiated on the surface of a cloud, the propagating shock will focus and produce large local pressure pulses and radiated acoustic pulses. It is not, however, clear exactly what form the foci might take in the highly non-uniform, three-dimensional bubbly environment of a cavitation cloud, for example, in a pump.

Experiments with hydrofoils experiencing cloud cavitation have shown that very large pressure pulses occur within the cloud and are radiated away from it during the collapse process. Within the cloud, these pulses can have magnitudes as large as 10bar and durations of the order of 10^{-4}s . This suggests a new perspective on cavitation damage and noise in flows which involve large collections of cavitation bubbles with a sufficiently large void fraction (or, more specifically, a large enough β) so that the bubbles interact

and collapse coherently. This view maintains that the cavitation noise and damage is generated by the formation and propagation of bubbly shock waves within the collapsing cloud. The experiments reveal several specific shock wave structures.

The phenomena described are expected to be important features in a wide range of cavitating flows. However, the analytical results clearly suggest that the phenomena may depend strongly on the cloud interaction parameter, β . If this is the case, some very important scaling effects may occur. It is relatively easy to envision a situation in which the β value for some small scale model experiments is too small for cloud effects to be important but in which the prototype would be operating at a much larger β due to the larger cloud size (assuming the void fractions and bubble sizes are comparable). Under these circumstances, the model would not manifest the large cloud cavitation effects which could occur in the prototype.

It is also the case that experimental observations of cloud cavitation in pumps are very limited though Soyama *et al.* (1992) conducted a valuable experiment that demonstrated the existence and importance of the phenomenon in a centrifugal pump. In this paper we have added some different and detailed observations of what we believe is a similar phenomenon in a wastewater pump and have identified some key vibration characteristics that might help the diagnosis in other applications.

In conclusion, these recent investigations provide new insights into the dynamics and acoustics both of individual cavitation bubbles and of clouds of bubbles. These insights allow tentative identification of the phenomenon in other practical contexts. The insights also suggest new ways of modifying and possibly ameliorating cavitation noise and damage.

5 Acknowledgements

My sincerest thanks to the graduate students and post-doctoral fellows who contributed to the results described, Luca d'Agostino, Douglas Hart, Sanjay Kumar, Beth McKenney, Yi-Chun Wang, Garrett Reisman, Fabrizio d'Auria, Mark Duttweiler, Al Preston and Keita Ando as well as to my colleague Tim Colonius. I am also most grateful for the support of the Office of Naval Research who sponsored much of the research described. I am also grateful to co-workers who provided help and information on the wastewater pump.

6 References

- Arndt, R.E.A., Ellis, C.R. and Paul, S. (1993). Preliminary investigation of the use of air injection to mitigate cavitation erosion. *Proc. ASME Symp. on Bubble Noise and Cavitation Erosion in Fluid Systems*, **FED-176**, 105–116.
- Bark, G. (1985). Developments of Distortions in Sheet Cavitation on Hydrofoils. *Proc. ASME Int. Symp. on Jets and Cavities*, 470–493.
- Bark, G., and Berlekom, W.B. (1978). Experimental Investigations of Cavitation Noise. *Proc. 12th ONR Symp. on Naval Hydrodynamics*, 470–493.
- Brennen, C.E. (1995). *Cavitation and bubble dynamics*. Oxford University Press.
- Brennen, C.E., Colonius, T., d'Auria, F. and Preston, A. (1998). Computing shock waves in cloud cavitation. *Proc. CAV98 Third Int. Symp. on Cavitation, Grenoble, France*.
- Chahine, G.L. (1982). Cloud cavitation: theory. *Proc. 14th ONR Symp. on Naval Hydrodynamics*, 165–194.
- d'Agostino, L. and Brennen, C.E. (1983). On the acoustical dynamics of bubble clouds. *ASME Cavitation and Multiphase Flow Forum*, 72–75.
- d'Agostino, L. and Brennen, C.E. (1988). Acoustical absorption and scattering cross-sections of spherical bubble clouds. *J. Acoust. Soc. of Amer.*, **84**, No.6, 2126–2134.

- d'Agostino, L. and Brennen, C.E. (1989). Linearized dynamics of spherical bubble clouds. *J. Fluid Mech.*, **199**, 155–176.
- de Lange, D.F., de Bruin, G.J. and van Wijngaarden, L. (1994). On the mechanism of cloud cavitation - experiment and modeling. *Proc. 2nd Int. Symp. on Cavitation, Tokyo*, 45–50.
- Franc, J.P., and Michel, J.M. (1988). Unsteady Attached Cavitation on an Oscillating Hydrofoil. *J. Fluid Mech.*, **193**, 171–189.
- Hanson, I., Kedrinskii, V.K. and Mørch, K.A. (1981). On the dynamics of cavity clusters. *J. Appl. Phys.*, **15**, 1725–1734.
- Hart, D.P., Brennen, C.E. and Acosta, A.J. (1990). Observations of cavitation on a three dimensional oscillating hydrofoil. *ASME Cavitation and Multiphase Flow Forum*, **FED-98**, 49–52.
- Knapp, R.T. (1955). Recent investigations of the mechanics of cavitation and cavitation damage. *Trans. ASME*, **77**, 1045–1054.
- Kubota, A., Kato, H., Yamaguchi, H. and Maeda, M. (1989). Unsteady structure measurement of cloud cavitation on a foil section using conditional sampling. *ASME J. Fluids Eng.*, **111**, 204–210.
- Kubota, A., Kato, H. and Yamaguchi, H. (1992). A new modelling of cavitating flows - a numerical study of unsteady cavitation on a hydrofoil section. *J. Fluid Mech.*, **240**, 59–96.
- Kumar, S. and Brennen, C.E. (1991). Non-linear effects in the dynamics of clouds of bubbles. *J. Acoust. Soc. Am.*, **89**, 707–714.
- Kumar, S. and Brennen, C.E. (1992). Harmonic cascading in bubble clouds. *Proc. Int. Symp. on Propulsors and Cavitation, Hamburg*, 171–179.
- Kumar, S. and Brennen, C.E. (1993). Some nonlinear interactive effects in bubbly cavitation clouds. *J. Fluid Mech.*, **253**, 565–591.
- Le, Q., Franc, J. M. & Michel, J. M. (1993). Partial cavities: global behaviour and mean pressure distribution. *ASME J. Fluids Eng.* **115**, 243–248.
- McKenney, E.A. and Brennen, C.E. (1994). On the dynamics and acoustics of cloud cavitation on an oscillating hydrofoil. *Proc. ASME Symp. on Cavitation and Gas-Liquid Flows in Fluid Machinery and Devices*, **FED-190**, 195–202.
- Mørch, K.A. (1980). On the collapse of cavity cluster in flow cavitation. *Proc. First Int. Conf. on Cavitation and Inhomogenities in Underwater Acoustics, Springer Series in Electrophysics*, **4**, 95–100.
- Mørch, K.A. (1981). Cavity cluster dynamics and cavitation erosion. *Proc. ASME Cavitation and Polyphase Flow Forum*, 1–10.
- Mørch, K.A. (1982). Energy considerations on the collapse of cavity cluster. *Appl. Sci. Res.*, **38**, 313.
- Omta, R. (1987). Oscillations of a cloud of bubbles of small and not so small amplitude. *J. Acoust. Soc. Am.*, **82**, 1018–1033.
- Reisman, G.E., Wang, Y.-C. and Brennen, C.E. (1998). Observations of shock waves in cloud cavitation. *J. Fluid Mech.*, **355**, 255–283.
- Shen, Y., and Peterson, F.B. (1978). Unsteady Cavitation on an Oscillating Hydrofoil. *Proc. 12th ONR Symposium on Naval Hydrodynamics*, 362–384.

- Shen, Y., and Peterson, F.B. (1980). The Influence of Hydrofoil Oscillation on Boundary Layer Transition and Cavitation Noise. *Proc. 13th ONR Symposium on Naval Hydrodynamics*, 221–241.
- Soyama, H., Kato, H., and Oba, R. (1992). Cavitation Observations of Severely Erosive Vortex Cavitation Arising in a Centrifugal Pump. *Proc. Third IMechE Int. Conf. on Cavitation*, 103–110.
- Sturtevant, B. and Kulkarny, V.J. (1976). The Focusing of Weak Shock Waves. *J. Fluid Mech.*, **73**, 651–680.
- Ukon, Y. (1986). Cavitation characteristics of a finite swept wing and cavitation noise reduction due to air injection. *Proc. Int. Symp. on Propeller and Cavitation*, 383–390.
- van Wijngaarden, L. (1964). On the collective collapse of a large number of gas bubbles in water. *Proc. 11th Int. Conf. Appl. Mech.*, Springer-Verlag, Berlin, 854–861.
- Wade, R.B. and Acosta, A.J. (1966). Experimental Observations on the Flow Past a Plano-Convex Hydrofoil. *ASME J. Basic Eng.*, **88**, 273–283.
- Wang, Y.-C. and Brennen, C.E. (1995a). The noise generated by the collapse of a cloud of cavitation bubbles. *Proc. ASME/JSME Symp. on Cavitation and Gas-Liquid Flow in Fluid Machinery and Devices*, **FED-226**, 17–29.
- Wang, Y.-C. and Brennen, C.E. (1995b). Shock wave and noise in the collapse of a cloud of cavitation bubbles. *Proc. 20th Int. Symp. on Shock Waves*, 1213–1218.